Keynote

20-23 June 2021

Time and Frequency Domain Transformations in the Structural Identification

Kemal Beyen

Professor, Kocaeli University, Kocaeli, Turkey
Corresponding Author E-mail: kbeyen@kocaeli.edu.tr

Corresponding Author ORCID: 0000-0001-8878-0985

Keywords

Time domain,
Frequency domain,
Structural health monitoring (SHM),
Transformation methods,
Time-Frequency,
Crack initiation,
Flaw initiation.

Abstract

This research reviews the development and application of time domain and frequency domain transformations in the field of structural identification and particularly in the structural health monitoring (SHM) practices in the last half century. The challenges in conventional transformations and future trends are discussed in the light of the development of Time-Frequency domain techniques for the SHM of civil engineering structures. Fourier Transform, short time Fourier transform, Laplace transform, Wavelet transforms, and Hilbert transforms are exemplified as some currently used transformations in data mining studies in engineering practice. This presentation also reviews the basic principles of the transformation methods, which open new spectral view in understanding and feature extraction methodologies. The SHM operation covers the operational evaluation during monitoring the structure, data acquisition, fusion, cleansing, feature extraction, and decomposition. Time-Frequency approaches show that structural parameters are changing as observed from field measurements, values of the parameters are varying through the time recorded on real structures under constructed conditions with natural environment. Using Time-Frequency analysis techniques, system identification on a real structure may give the possibility to trace the signals to identify the structural damage and progressive deterioration including the detection of damage source and partially collapse mechanism. If instrumentation is dense enough, in local scale, in case of over member capacity exceedance, it may become possible that the priory condition before the crack or flaw initiation is detected at the available earliest stage. Based on the author's experience in the field, examples of results obtained from studies conducted over the years will be presented in this study.

1. Introduction

In building codes, performance-based design of a new structure and assessment of the existing building that are consist of nonlinear dynamic analysis eventually demonstrate the potential of nonlinearity and nonstationary characteristics in structural responses [1]. Furthermore, with new energy dissipation technologies and strategies, instead of strengthening whole members to resist deformations under earthquake loads, designing structure with the replaceable fuse elements like special devices or weaken beams needs nonlinear dynamic analysis too. So, the suggested damage control approach can dissipate propagating earthquake energy by yielding beams or failing devices and reduces the stress on the more crucial structural members like columns and shear walls. Structures with dampers or base isolation systems designed to reduce the incoming input motion at the base level or minimizes the member forces and deformations in the structure that can be counted as innovative systems should be analyzed with nonlinear dynamic analysis [1]. Or recently emerging developments like architectural aseismic building design to keep the nonstructural members functioning after an earthquake. Failure of non-structural components (i.e., falling panels, windows, collapse of the ceiling as interior damage or falling curtain walls or panels as exterior damage). Collapse potential of such components of the ordinary buildings or industrial structures can be identified after performing a series of nonlinear dynamic analysis. For this purpose, dynamic inelastic response history analysis is essential to determine member forces and deformations. Nonlinear dynamic analysis is one of the accurate estimation methods for evaluating the response of structures when subjected to earthquake. Nonlinear simulations that are closer to the real behavior include nonlinear analysis based on incremental plastic theory for different global performance levels of a structure. In real dynamic behavior, structure redistributes the forces due to yielding members. This force redistribution progressively effects the stress state and introduce nonstationary characteristic. Furthermore, in the case where nonlinear analysis is performed in the time domain, the dynamic behavior should be defined through relevant literature and specifications with proven theoretical and experimental validations [1]. On the other hand, selection of the methodology in conventional approaches limits the engineers to linear elastic based approaches. Further studies required for better understanding damage and ductile performance show the necessity of the time-frequency analysis. Damage susceptibility or performance estimates of structures that were obtained by applying the time-frequency techniques to nondestructive test data or virtual simulations based on numerical modelling were verified later by the earthquake damage survey [2]. Deformation based design and assessment as proposed by the new generation building codes is an important step in structural analysis. Traditional building codes use simplified linear or empiric expressions proposed based on observations that aim to estimate some limit values for design parameters and let the structure to be in safe side. This epistemic uncertainty can be called as 'deterministic'. For instance, for a more refined analysis considering the nonlinear elastic behavior of structural system, the second order effects in nominal ductility level is not mandatory up to code proposed critical limit. Building codes overlook the deformation geometry under design earthquake spectra, which is estimated to include random nature of ground motions. In a simple scenario for a safe service life, modelling an engineering structure is controlled by an estimated return period and spectral amplitudes in case of frequency domain approaches or a set of intensive earthquake data in case of nonlinear time history analysis. In the service life of the structure, structure may produce varying responses to such randomly changing natural forces. This study particularly suggests that the results inferred separately from time domain and frequency domain may be visualized together in the frequency-time plane to better understand the structural condition

and its response characteristics. One of several objectives of this paper is to establish or initiate a risk consistent structural analysis in time-frequency domain. The future revisions of aseismic design and condition assessment can recommend the time frequency domain analysis for a consistent design to account the chaotic natural forces and resultant structural responses.

Regarding widely used algorithms, structural identification and as well as damage identification methods can be roughly classified into categorized index methods, calibration-based model updating methods, and vibration signal-based methods [3, 4, 5]. Each identification method requires modal properties of the structural system. With the developing observation technologies, signal-based identification studies and damage assessment methods give comprehensive global information from in-situ measurements. The experimental studies can also be extended to modal identification studies including model verification and, if necessary, numerical model calibrations with respect to the findings inferred from in-situ measurements. Of course, under linear elastic conditions, modal properties in cases of theoretical free vibration and operational vibrations are certainly estimated from recorded vibration data using conventional Fourier transforms (FT) [2, 5].

FT decomposes a signal by a linear combination of projections onto an infinite length and transforms energy content in terms of harmonics (i.e., sinus as y axis projection and cosines as x axis projection in complex plane). However, it is unable to capture local features. Due to random nature of the ground motion, perfect harmony between the application norms of the FT and characteristics of the natural events is not seen in most cases. There are a few inherent characteristics of FT that might affect the accuracy of system identification and damage detection. Firstly, due to performing average over the time, the FT smooths the amplitude and assigns the single average amplitude at each frequency, while same frequency signals may be observed with different amplitudes at different instants of time in the record. Recorded data inherently holding the information about the structural behavior might be lost or deteriorated during this severe averaging process. Misinterpretation of such results due to weaken signal statistics might be another risk at the stage of structural evaluation. Such lost may affect the outcomes of the further analyses and may remarkably mislead the decision for the condition assessment. Verifiable such facts show that FT is not able to present the time dependency information of the signals because there is no time memory [2, 5]. Essentially when the inverse Fourier Transform is performed, same frequency signal with different amplitudes cannot be replaced back to their time stations in the original record, because there will be only one average amplitude with single frequency. Second, damage is a local phenomenon which tends to be detected in higher frequencies as studied by Beyen, K. [2, 5]. These higher frequencies that are closely spaced are poorly excited by low data in the noise band. FT is not sensitive to small changes in time series. For instance, a small frequency change in Fourier transform will result in changes in the time data. However small amplitude change like spike in the time series will not change the amplitudes in Fourier amplitude spectrum due to averaging. All these factors introduce some difficulties. Therefore, damage identification methods based on FT may not be suitable. To challenge such problems, two approaches among several in recent years have received increasing attention; they are the wavelet transform and empirical mode decomposition with Hilbert transform. In several studies, their superior performances were comparatively discussed for frequency content change over time due to nonstationary data characteristic [2]. To localize frequency content in time, a time-frequency map for nonstationary data was developed. Wavelets can change locally in both frequency and time domain, and the memory of time location provides great difference and produces numerous advantages in identification studies. Another difference is that wavelet with suitable mother function offers a comprehensive form to approximate the target function, but Fourier transform cannot. To overcome such shortcomings, signal-based transformations were improved and applied in literature [2, 7, 8]. They are, chronologically, Short Time Fourier transform (STFT), Laplace transform (LT), Wavelet transform (WT), Hilbert transform (HT) and Hilbert Huang Transform (HHT) among several to be mentioned and will be discussed in this study. Some of them were improved by the time like STFT and HHT [2]. The last one was developed by Huang et al. [9] and has been preferred as comprehensive application in the SHM in the last two decades. Huang et al. [2, 9, 10] firstly proposed a new algorithm named empirical mode decomposition (EMD) for analyzing nonlinear and nonstationary data. The most pioneering idea is the introduction of adaptive EMD method, which produces finite number of intrinsic mode functions (IMF) based on local averages from maxima and minima through the time axis. With such IMFs, Hilbert transform satisfy the theoretically working conditions and admit well-behaved HT. Since then, the method was mentioned Hilbert-Huang Transform (HHT) and has been adopted in many engineering disciplines to give new insights into the nonstationary and nonlinear physical phenomena [2, 5, 9, 10]. Application of HHT to SHM was firstly investigated by Vincent et al. [11] and then Yang et al. [12] used HHT to carry out the system identification and damage detection. HHT based approaches in the structural health monitoring (SHM) has attracted more attention and a great number of studies can be found in the literature for the aspects of theory and field tests. Nevertheless, there are still many difficulties and challenges concerning the HHT based identification in civil engineering practices. This presentation reviews the developments in identification methods in the recent decades and applicability of the traditional and new techniques in the field of SHM. Real examples are selected to show the strengths and weaknesses of the methods. In-situ measurements recorded on concrete-reinforcement bending moment shear frame tower from 20th Century and stone masonry built historical structure from 15th Century are studied to demonstrate the sensitivity level of the structural identification and damage detection. Finally, the challenges and future trends in different techniques for structural health monitoring are shortly discussed.

2. Signal processing for damage detection

Damage may be caused from many reasons like any deviation in the geometric or material properties of a structure. These deviations may have an adverse effect on current or future performance of the structure. These deviations may develop due to a variety of reasons such as; (i) degradation of material properties, like cracking, corrosion, fatigue and plasticity; (ii) fabrication errors like cracks, voids, flaws and spots; (iii) loosening structural connections like bolts and broken welds; (iv) construction errors like improper assembly or misfits [13]. Therefore, (v) change in geometric properties or loss of structural strength or capacity exceedance due to operational factors [3]. Depending on the level of intensity and cause of the damage, damage pattern may vary due to operational and environmental factors. Damage usually starts at the material level and extents from microscopic scale to the global scale at anywhere from minor to severe in the structure, and may accumulate incrementally over long time period such as fatigue or corrosion and eventually progressive degradation causes failure if the damage remains undetected. In order to detect damage at an early stage, suitable damage identification methods should be selected. Most of the damage identification methods use signals as input-output couples that may be recorded synchronically during natural events such as earthquake, wind or blast pressure as input data and resultant acceleration, displacement or strains as output responses. Signals, which may be stationary or non-stationary, affect the selection of the processing technique in identification analysis. Stationary signals do not change their characteristics with the time, while nonstationary signals change their characteristics (i.e., for instance, mean values taken for short time windows through the record length, if show stable mean, signal is accepted to be stationary, otherwise signal is considered nonstationary). Signals whose frequency content do not change in time are called stationary signals. In other words, the frequency content of stationary signals does not change in time. In this case, one does not need to know at what times frequency components exist, since all frequency components exist at all times.

3. Conventional signal processing

It is an observable fact that the dynamic systems do not produce responses in a linear way. Structural system instantly modifies the input excitation propagating through the structure from base and the structure synchronously modifies its responses. Therefore, nonlinear behavior is a usual situation rather than the linear behavior, and the adaptive structural responses produced by the instantaneously changing input forces introduce the non-stationary feature into the records. Since the design parameters of the structure and local environmental conditions may change by the time, such dynamic systems cannot be identified appropriately. Consequently, using in-situ measurement data, simple linear representative systems like lumped mass model are adopted for simulations. In linear time domain simulation studies, single-input single-output (SISO) model, multi-input, multi-output (MIMO) models and single input multi-output (SIMO) mathematical (i.e., parametric) models have been used in many system identification studies. Using parametric models,

transfer functions estimated based on field measurements may also predict the structural behavior of the SISO, MIMO or others for the test building. Transfer function in this case can be efficient and powerful estimation tool to understand better the performance of the structural system. This parametric identification is suitable only for linear and stationary dynamics [2, 4, 5, 7, 8]. In case of nonlinearity and nonstationary dynamic, Time Frequency (T-F) algorithms can be preferred. Based on in-situ measurements, estimated Frequency Response Function (FRF) can also be used for feature extraction of a structure and for damage detection as well [8]. Within the time domain methods, among several techniques, Eigen system Realization Algorithm (ERA) techniques can be mentioned as one of the most widely used approaches. ERA with Observer Kalman Identification method (OKID/ERA) [2, 7, 8, 14, 15] based on the concepts of the control theory is a more general approach for handling the effect of noise and numerical errors in advanced modal parameter identification techniques [16].

4. Spectral method in damage ıdentification

In general, ambient vibration data that is recorded on the structure hold low amplitude structural vibration signal and large amplitude wide-band noise. Therefore, in case of damage identification, Fourier based spectral methods are usually not suitable if filtering processing is not applied precisely for signal to noise ratio low measurements. Using test data, time domain system identification technique or equivalently frequency response of the structure may provide valuable insight and represent well enough underlying dynamics of the structure if sampling and recording time are suitable [17].

FRF (H(w)) describes the relationship as the Fourier amplitude ratio between FT of the output response of a structure (*Y(t)*) and FT of the excitation force (*F(t)*) at the free field, as seen in Eq (1a). Applying FT to the cross (R_{FY}) and auto (R_{FF} and R_{YY}) correlations, spectral density functions (S_{FY}, S_{FF}, S_{YY}) can also be used in order to minimize the effects of noise on the output, as seen in Eq(1b) defined as *H1(w),* and another alternative noise minimization if performed to the input data as seen in Eq(1c) defined as H2(*w*); all may be defined as followings [5, 8].

$$H(w) = \frac{Y(w)}{F(w)} \tag{1a}$$

$$H_1(w) = \frac{S_{FY}(w)}{S_{FF}(w)} \tag{1b}$$

$$H_2(w) = \frac{S_{YY}(w)}{S_{YF}(w)} \tag{1c}$$

5. Time domain (OKID/ERA) method

OKID/ERA algorithm based on state-space model, coded in Matlab [2, 5, 14, 15, 16] is composed of the following three major computational steps: (1) The observer Markov parameters are calculated with OKID. (2) From the observer Markov parameters, OKID, this time, retrieves the system Markov parameters. (3) ERA is utilized with the system Markov parameters to realize the discrete time state-space (*SS*) system matrices, *A*, *B, C* and *D*. Markov parameters forming the basis for identifying mathematical models are the unit sample response or pulse response histories of the system. In the classical approach, Markov parameters might be extracted from inverse Fourier Transform (IFT) of the frequency response function (FRF), which is defined as the ratio of the Fourier Transforms (FT) of the measured output and input data. Due to aliasing and numerical ill-conditioned problems, calculating accurate Markov parameters in this way is impractical. FT algorithm requiring appropriately long-time histories has another disadvantage in calculations. In contrast to the classical technique, OKID finds the Markov parameters more quickly and accurately than FFT-IFFT. Moreover, since OKID has an asymptotically stable observer, influence of the noise and other problems appearing in the estimation of the system Markov parameters from direct input-output data are bypassed. Further details of the theory with derivations are described in Juang.' [2, 5, 14, 15, 16].

6. Time-frequency analysis

T-F decomposition shortly maps a one-dimensional signal into a two-dimensional signal and describes how the spectral content (i.e., frequency and phase) changes with the time. If FT is considered as the first in the chronological order in transformation calculations; As the first shortcoming, the Fourier transform can only be applied to time series with stationary and linear properties. However, as discussed earlier, due to earthquake or wind, structural responses recorded on civil infrastructure are mostly nonstationary. The second inadequacy of the Fourier analysis is that it cannot give the time dependent frequency and phase changes. In fact, operational quantities are very important in structural health evaluations in time-frequency domain. The third inadequacy is that the Fourier transform is not applicable to response records of a structure because the structure may continuously receive instant member capacity exceedances or member failures during the earthquake. Fourier transforms (FT) and invers Fourier transform (IFT) can be expressed respectively, as

$$F(w) = \int_{-\infty}^{\infty} f(t)e^{-i\omega t}\,dt \qquad f(t) = \int_{-\infty}^{\infty} F(w)e^{i\omega t}\,dw \tag{2}$$

where ω is the angular frequency and $F(\omega)$ is essentially complex. As seen from Eq. (2), FT decomposes the signal down to the sinusoids that theoretically extend from minus to plus infinity unlike the real-world physics' condition. In contrast to infinitely oscillating sub-harmonics of the FT, frequency of an irregular and almost non-symmetrical wavelet varies over the length of the waveform and it is better at describing non-stationary problems. A wavelet has an amplitude that starts out at zero, increases and then decreases back to zero within a certain time span. By stretching (dilating) and shifting (translating) the waveforms, wavelets that come in various shapes and sizes are used to detect the hidden event and approximate its frequency and location in time. A specific mother wavelet shape that may match or correlate the time series unusually well when the mother wavelet is stretched and shifted. Even if a wavelet is transformed from time domain into frequency domain, still the relative phase relations of different contributing frequencies determine the position in time.

6.1. Short time frequency transforms

Focusing on the localization in time and frequency is at least not the only property that is characteristic about the wavelet transform. Much earlier, short-time Fourier transform (STFT) that is also localized in time and frequency is introduced to overcome the limitations of the FT by Gabor [10, 17] and using Gaussian (normal distribution function) window *g(t)*, it provides information about where in time a certain frequency occurs, since it is essentially collection of the FTs applied consecutively onto the windowed (i.e., small) portions of the signal. The signal in the sliding small time window is assumed approximately stationary. Using the inner product notation, the STFT can be expressed as

$$STFT(\tau, f) = \int x(t)g(t-\tau)e^{-i\omega t}dt \tag{3}$$

STFT employs a sliding window function *g(t)* centered at time τ of the window. FT is performed on the signal *x(t)* within the window. Through such consecutive operations, FT of the entire signal decomposes into a two-dimensional T-F representation. Recorded field data is generally not known a priori, selection of a suitable window size for effective signal decomposition or for processing nonstationary events in the STFT is difficult.

6.2. Wavelet transforms

In contrast to the STFT where the sliding time window size is fixed and is not suitable for nonstationary data, the wavelet transform enables flexible window sizes in analyzing different frequency components within a signal. By comparing the level of similarities between the signal and a set of patterns obtained from dilating and contracting the original period (i.e., scaling represented by *s*) and translating along the time axis (i.e., shifting, τ) of a base wavelet $\psi(t)$, T-F characteristic may be mapped remarkably. Using inner product, the wavelet transforms (WT) of a signal *x(t)* can be expressed as;

$$wt(s,\tau) = \frac{1}{\sqrt{s}}\int_{-\infty}^{\infty} x(t)\psi^*\left(\frac{t-\tau}{s}\right)dt \tag{4}$$

where the scaling parameter, *s* greater than zero, which determines the time and frequency resolutions of the scaled base wavelet $\psi\langle(t-\tau)/s\rangle$. The specific values of *s* are inversely proportional to the frequency. The symbol $\psi^*(\cdot)$ denotes the complex conjugate. WT can extract the inherent components within time series over its entire spectrum, by using small scales (corresponding to higher frequencies)

and large scales (corresponding to lower frequencies) for decomposing frequencies. The scaling factor controls the amplitude of the wavelet function, and the time shift controls the location of the wavelet function on the time scale. As the scaling factor changes, the effective width of the wavelet function will change. Unlike Fourier transforms, wavelet transforms can meet the requirements of the problems observed in monitoring studies. For example, the wavelet transforms produce rich time resolutions, depending on the frequency components [9, 10]. Advantageous of the wavelet transforms may be summarized as followings: (*i*) Mathematically well developed and ready to apply to great number of problems, (*ii*) inverse transforms exist, (*iii*) both continuous and discrete forms exist, (*iv*) practically, transformation does not have any limit for frequency and time resolutions, (*v*) they are applicable to nonstationary data and nonlinear engineering problems, (*vi*) contrast to FT that can give only mathematical result, Wavelet transforms have direct applications in structural damage detection such as identification by the wavelet spectrum, as well as singular signal detection, WT can also be used as the noise filter, frequency-band analysis and so on. Numerical results performed for a minor localized damage can induce notable changes in the wavelet coefficients of the structural data. Recent wavelet-based approach is studied by the author to identify the global anomaly and to locate the damage in civil engineering structures, on the basis of the acceleration responses [2, 5]. Using available different conventional and new identification techniques, for both the undamaged and damaged reinforced concrete frame structure. The features of the structure and identification sensitivity are studied. Regardless of the excitation mechanism, identification process is entirely based on the measured responses. In order to increase the accuracy in damage localization in complex structures, well instrumented SHM network is necessary.

6.3. **Hilbert–huang transform**

The Hilbert–Huang transform (HHT) that is an empirical approach solves the nonstationary data, based on the Hilbert transform, has become very popular method in signal processing [9]. The Hilbert transform is defined, for an arbitrary time signal *x*(*t*) with the Cauchy principal value *P*, as

$$H[c_i(t)] = \frac{P}{\pi}\int \frac{c_i(u)}{t-u}\,du \tag{5}$$

Huang uses self-adaptive empirical mode decomposition (EMD) to decompose a signal into some number of intrinsic mode functions (IMF) based on the technique as he proposed. Then HT is applied to the IMF to obtain instantaneous frequency and phase information. Since the signal is decomposed in the time domain within the original length of the real-world signal having nonzero mean and nonstationary characteristics. Separated interferences (IMF) with zero mean can be associated with a physical meaning. Furthermore, these IMFs can also provide the modal data (i.e., modal frequencies, damping ratios and mode shapes). Story stiffness can be obtained if instrumentation layout is set up the whole floors. Story damage can then be detected by comparing the stiffness values of identical floors. HHT offers many advantages over the other techniques, such as (*i*) applicable to nonstationary signals and nonlinear problems, (*ii*) producing more physically meaningful results than those offered by other transforms, and (*iii*) suitable to produce adequate frequency and time resolution to engineering problems within the time and frequency ranges of interest. (*iv*) Although the wavelet transforms are applicable to nonstationary signals and nonlinear systems. Results offered by the wavelet can only give indication of damage as side effects, therefore, the wavelet transforms are not adaptive. Beside all the advantages of the wavelet transforms, HHT has the property of additivity. That additivity can produce more physically meaningful results and provides characteristic frequency and time resolution for the structure. Steps are summarized below, and details may be found in Huang et al. [9]. The EMD was designed based on the assumption that the data set consists of simple different intrinsic mode functions (IMF) of oscillations with harmonic or nonsinusoidal coexisting characteristics derived recursively from the data. First mean m_1 is calculated and subtracted from the whole data, *X* and difference h_1 called IMF candidate as a first component since it satisfies all the conditions of an IMF as detailed in Huang et al. [9].

$$h_1(t) = X(t) - m_1(t) \tag{6}$$

However remaining data $h_1(t)$ that is treated as the recent data and previous process, called the sifting, is repeated;

$$h_{11}(t) = h_1(t) - m_{11}(t) \tag{7}$$

In this case, m_{11} becomes mean of the upper and lower envelopes of h_1. Consequently, other rounds of sifting process are carried out k times until the residue becomes constant (monotonic) or represents an ignorable trend (baseline passing from zero at most two times).

$$h_{1k}(t) = h_{1(k-1)}(t) - m_{1k}(t) \rightarrow c_1(t) = h_{1k}(t) \tag{8}$$

Then the recent $h_{1k}(t)$ is nominated as the first IMF component c_1, which contains highest frequency content of the signal *X(t)*. c_1 is removed from the data *X(t)* to obtain the residue r_1, which contains lower frequency components. The r_1 is treated as the new data and subjected to the same sifting process. This procedure is repeated to obtain all the subsequent r_i functions*;*

$$r_1(t) = X(t) - c_1(t) \rightarrow r_i(t) = r_{i-1}(t) - c_i(t),\ i = 2,3,4,\dots\dots,n \tag{9}$$

After completing the decomposition process, the original signal can be collected by summing n IMF components (i.e., $c_i(t)$), including the final residue $r_n(t)$.

$$X(t) = \sum_{i=1}^{n} c_i(t) + r_n(t) \tag{10}$$

In HSA, signal ci(t) and its HT, H[ci(t)] can be combined to form the analytical signal Zi(t) in a complex structure,

$$Z_i(t) = c_i(t) + j\,H[c_i(t)] = a_i(t)\,e^{j\theta_i(t)} \tag{11}$$

where P denotes the Cauchy principle value. With this newly defined analytical signal, time-dependent a(t) and phase $\theta(t)$ become observable over the time and the instantaneous frequency can be defined from 1st derivation of $\theta(t)$ with respect to the time as,

$$a_i(t) = \sqrt{{c_i}^2(t) + H[c_i(t)]^2} \tag{12a}$$

$$\theta_i(t) = arctan\,\frac{H[c_i(t)]}{c_i(t)} \tag{12b}$$

$$w(t) = \frac{d\theta(t)}{dt} \tag{12c}$$

Applying the HT to the *n* IMF components of X(t) but excluding nonzero pass residue r_n, X(t) can be written in terms of amplitude and instantaneous frequency corresponding to each component i as functions of time.

$$X(t) = \Re\ \sum_{i=1}^{n} a_i(t) e^{j\int w_i(t)dt} \tag{13}$$

Eq. (14) differs from the time-independent amplitude and phase in the FT. It improves the flexibility of the expansion and tracks the nonstationary characteristic. The T-F distribution of the amplitude called as the Hilbert spectrum *H(w,t)* defined as

$$H(w,t) = \sum_{i=1}^{n} \tilde{H}_i(w,t) = \sum_{i=1}^{n} a_i(t) \tag{14}$$

Where $\tilde{H}_i(w,t)$ stands for *i*th component of the total Hilbert spectrum *H*. The square of *H* also gives the energy distribution (i.e., energy density). Another very important definition is the marginal spectrum *h(w)* provides a measure of total amplitude contribution from each frequency, in which *T* denotes the time length of the signal.

$$h(w) = \sum_{i=1}^{n} \tilde{h}_i(w) = \sum_{i=1}^{n} \int_0^T a_i(t)dt \tag{15}$$

7. **Real case studies in structural analysis**

Real examples are selected to show the strengths and weaknesses of the conventional and new methods. In-situ measurements recorded on concrete-reinforcement bending moment shear frame tower from 20th Century and stone masonry built historical structure from 15th Century are studied to demonstrate the sensitivity level of the structural identification and damage detection.

7.1. **Structural identification and damage detection in historical masonry structure**

For ambient vibration measurements, 8 seismometers for two horizontal degrees of freedoms on the structural observation points and another one at the entrance of the structure were instrumented. For microtremor data, 1 seismometer as a free field measurement at

the ground was set for two horizontal degrees of freedoms as drawn in Figure 1. Locations of the sensors on the structure are key points believed to reflect the structural modal characteristics. The sensors, equipment and the data acquisition system can be found in reference [5]. The duration of the test measurement was 5 minutes. After structural measurements were completed, calibration test was also performed at the basement for whole equipment and sensors. Control test data were utilized for testing linearity and distortion in recordings based on high-resolution calibration procedure such as wavelet analysis. Finally, band pass filtering was decided between frequencies of 0.1 Hz and 50 Hz (as the Nyquist frequency) to eliminate the effects of white noise, hardware problems and effects of the different cable lengths. Base-line correction (linear and nonlinear if necessary) and resampling for eliminating high frequency spikes in the record were also performed when they were needed.

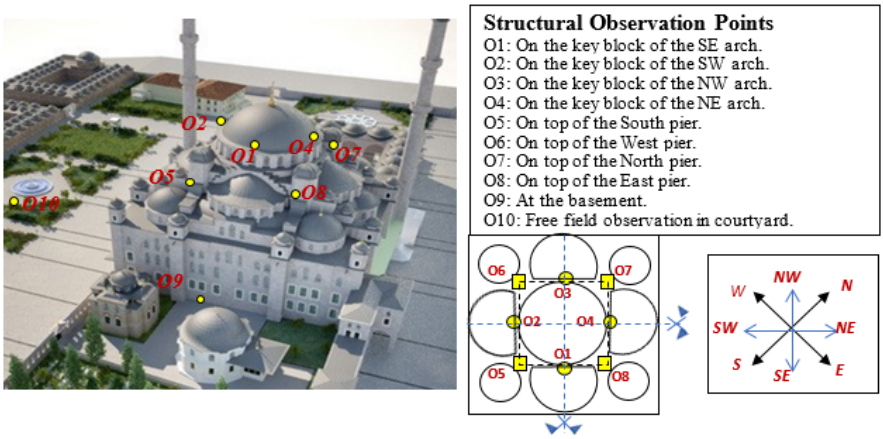

Figure 1. Seismometer locations from SE towards NW [2, 5].

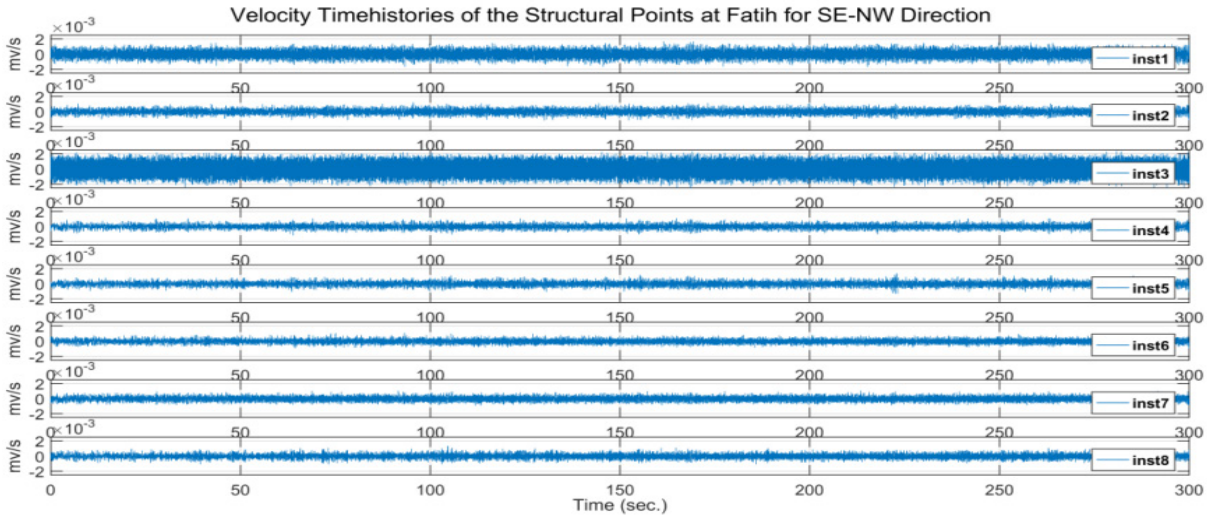

Figure 2. Velocity time histories for the structural observation points for SE-NW direction [5].

As a typical example, ambient velocity time histories of the structural points are plotted for SW-NE direction, as shown in Figure 2. Corrected data were Fourier transformed and smoothing was performed by SGolay filter with window length of 5 samples and polynomial degree of 2 for noise reduction without loss of high frequency content, which might hold structural information. Figure 3 shows the filtered Fourier amplitude spectra of the velocity time histories for the eight structural points. Denoising procedure based on Wavelet Decomposition was applied to ambient measurement data set. Details about the implementation and results that can be found in reference [5] manifest the data quality with reasonably high signal to noise rati

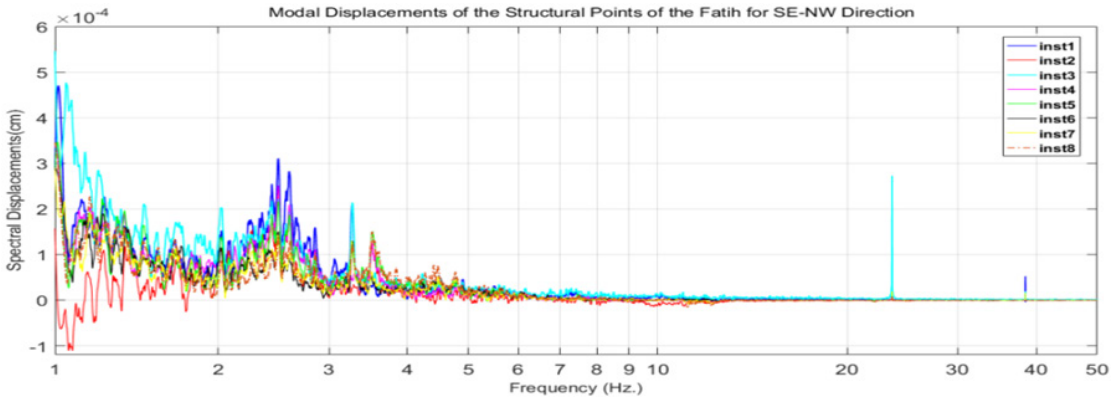

Figure 3. Spectral Displacements smoothed by Sgolay filter for SE-NW direction.

Transfer functions for SW-NE direction between the structural sensor points and the reference base have been calculated as plotted in Figure 4. Except the stations O1 and O3 that display significant shifts from 2.5Hz. to low frequency 1.8Hz., the spectral peaks at the cornice-level stations at the four springing points of the main arches and those at the crowns of the main arches at the dome-base occur almost at the same frequencies reflecting global response. For SE-NW direction, spectral peaks are observed at ~2.5, 3.5, 4.3, and 5.3 Hz. in Figure 4, it is obvious that station O3 with superior amplitudes and station O1 with relatively large amplitudes behave differently in both low and high frequency regions when compared within the group of other similar observation points for major directions. Stations O_3 and O_1 that envelope the others in the all frequency range have two sharp peaks with superior amplitude values at around 24Hz and 38Hz, respectively in high frequency region as seen in Figure 4.

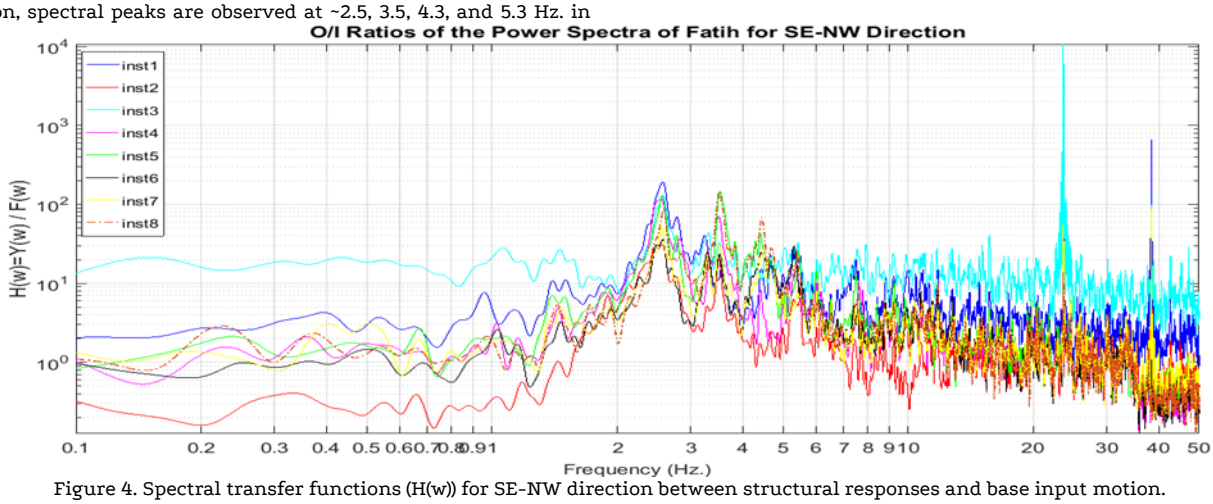

Figure 4. Spectral transfer functions (H(w)) for SE-NW direction between structural responses and base input motion.

In experimental modal identification, Single-Input Single-Output (SISO) transfer function and Multiple-Input Multiple-Output (MIMO) transfer function models and Observer/Kalman Filter Identification method with Eigen System Realization (OKID-ERA) technique [14, 15] were adopted, respectively in Figure 5 and 6. At the first modal frequency, four stations located at the crowns of the main arches have identical response except station 3 with less peak frequency and magnitude, as seen in Figure 6. Mode shapes of the structure have also been estimated by using the MIMO parametric model, which is equivalent to the MDOF system. Mode shapes are plotted in Figure 7 for the first five modes for both directions. Modal characteristics of the first five modes for each direction is also summarized in Table 2.

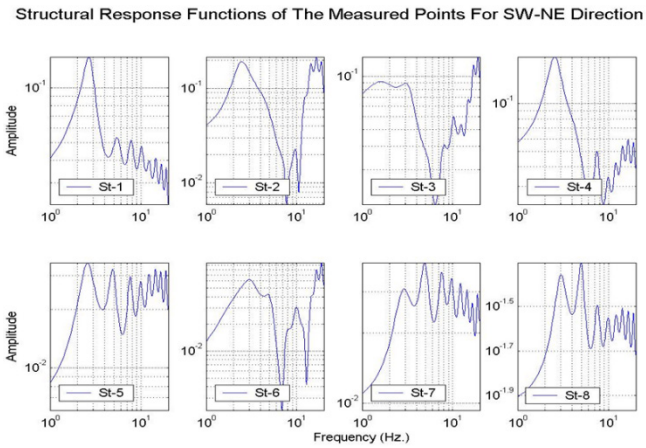

Figure 5. SISO transfer functions of the ARX structural models selected from many candidates based on the estimation performance for SW-NE direction [5].

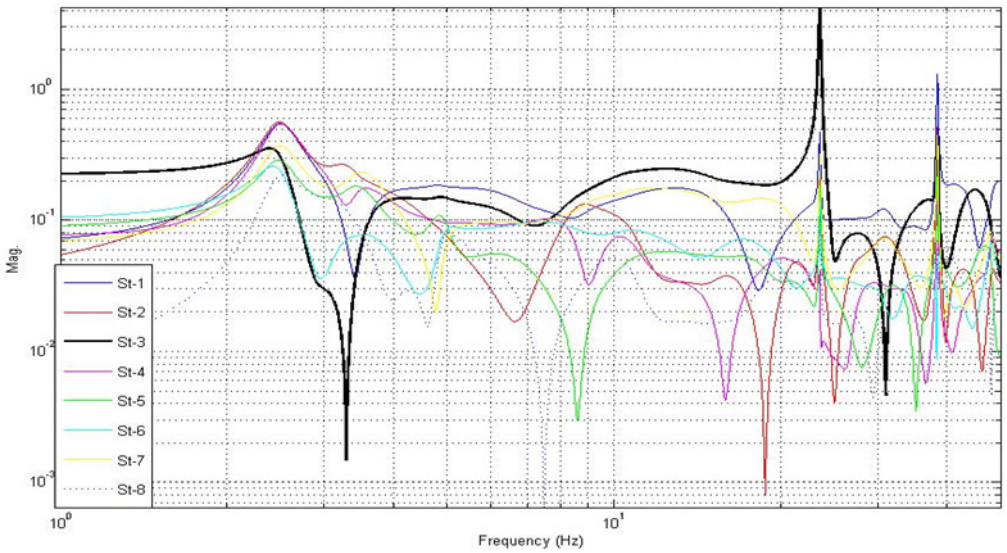

Figure 6. All transfer functions of the observation points for one data set for SW-NE direction estimated from the analysis of the MDOF system

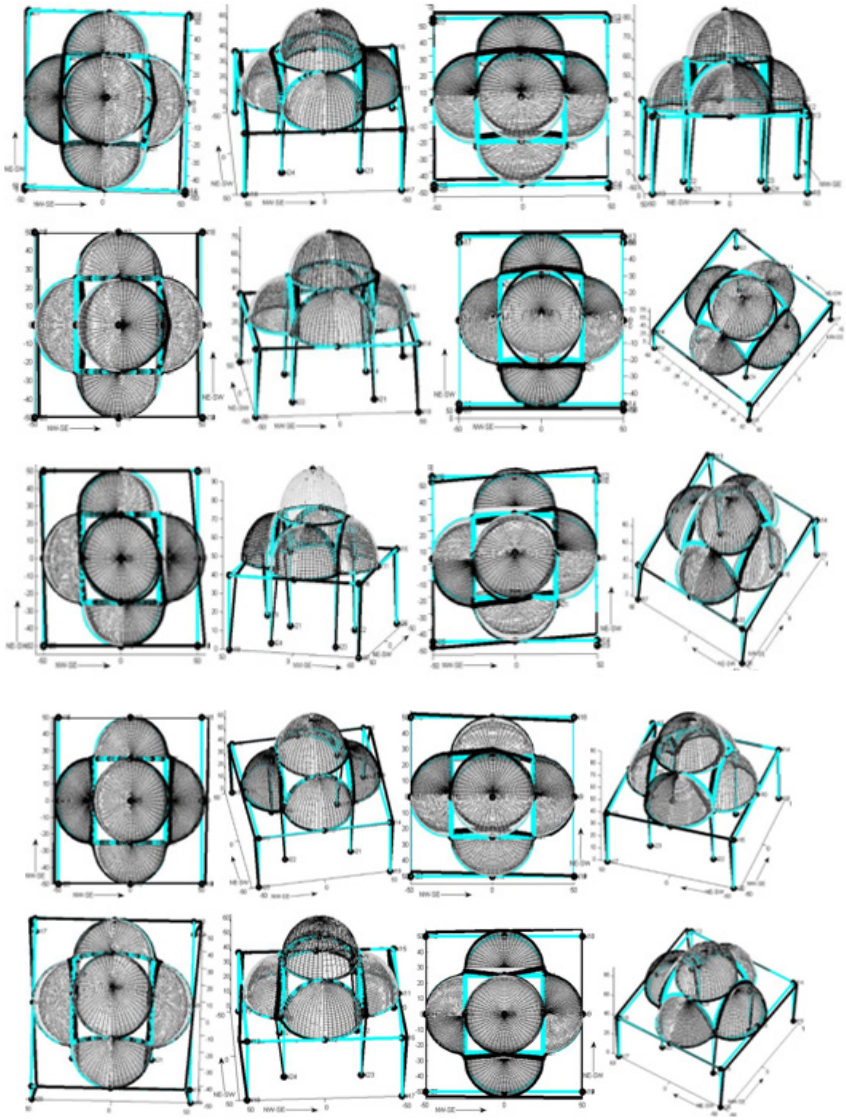

Figure 7. Exaggerated first five-mode shapes of the structure for both directions, namely SE-NW in left two columns and SW-NE in right two columns. Blue solid lines are for bare frame and black lines for modal deformations.

Table 2 Descriptions for first five modes in SE-NW and SW-NE directions

Modes	SE-NW Direction	SW-NE Direction
1st mode	Translation at the cornice level Breathing outwards at the base level of the dome @ 2.42 Hz	Total lateral vibration @ 2.31 Hz
2nd mode	Breathing inwards at the cornice level, swaying laterally at the level of the dome base @ 3.29 Hz	Breathing outwards @ 3.20 Hz
3rd mode	Squeezing vibration @ 3.52 Hz	Squeezing vibrations @ 3.38 Hz
4th mode	Breathing outwards @ 4.41 Hz	Total lateral vibration @ 4.04 Hz
5th mode	Antisymmetrically squeezing vibration @ 4.59 Hz	Breathing out at the cornice level, very small swaying laterally at the level of the dome base @ 4.47 Hz

Structural damages do not allow the structure to behave in a monotonic fashion and the measured data in either way yield similar results but different values of frequency shifts. Evidence of weak nonlinearity (residual deformation) observed by visual inspection is softly correlated by the results of the conventional techniques such as spectral and parametric analyses of both SISO and MIMO models. As alternative, STFT was computed by applying FT to a windowed segment of the data. STFT provides time-localized changes in frequency with limited precision and somehow reduces the nonstationarity but the window size influences the temporal and frequency resolution of the analysis. From STFT spectra in Figure 7, nonstationary characteristic can be observed on all observation points. However, at stations O_1 and O_3, two sharp spikes at 24Hz and 38Hz are developed exceptionally and they almost keep the linearity throughout the record length. Key block failure at O_3 and partial damage at O_1 may cause high frequency peaks indicating local damages. Due to poor redundancy as observed feature of the historical masonry structures, damage may destabilize the adjacent members in the SE- NW direction. This is seen globally on some neighbor members such as at O_2 and O_7 strongly and at O_6 slightly.

T-F spectra are estimated using wavelet theory for each direction. Several wavelet families are tested to extract the recognizable features for damage detection. Among many, bump wavelet base that is the most successful at identifying the damage is decided for this study. It is seen that local jump in the wavelet coefficients point out the location of the damage. Cross-examination of the T-F spectra among the stations can reveal localized similarities otherwise local increases in the absolute value of the wavelet coefficients may show nonstationary power in T-F plane. When the region has become full of high wavelet coefficients, nonlinear behavior experienced due to the interferences of the broken sides at the damage point and interactions between the adjacent components. Crown station O_3 in Figure 8 shows linearity throughout the recording with complete high power at around 24Hz in broadband characteristic. Severe damage at O_3 causes such linearity and loosens the bonds between the stones around the key block.

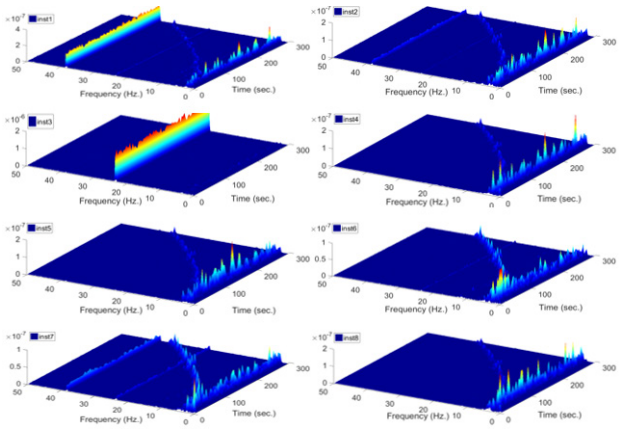

Figure 7 STFT of the records at the eight observation stations for SE-NW direction.

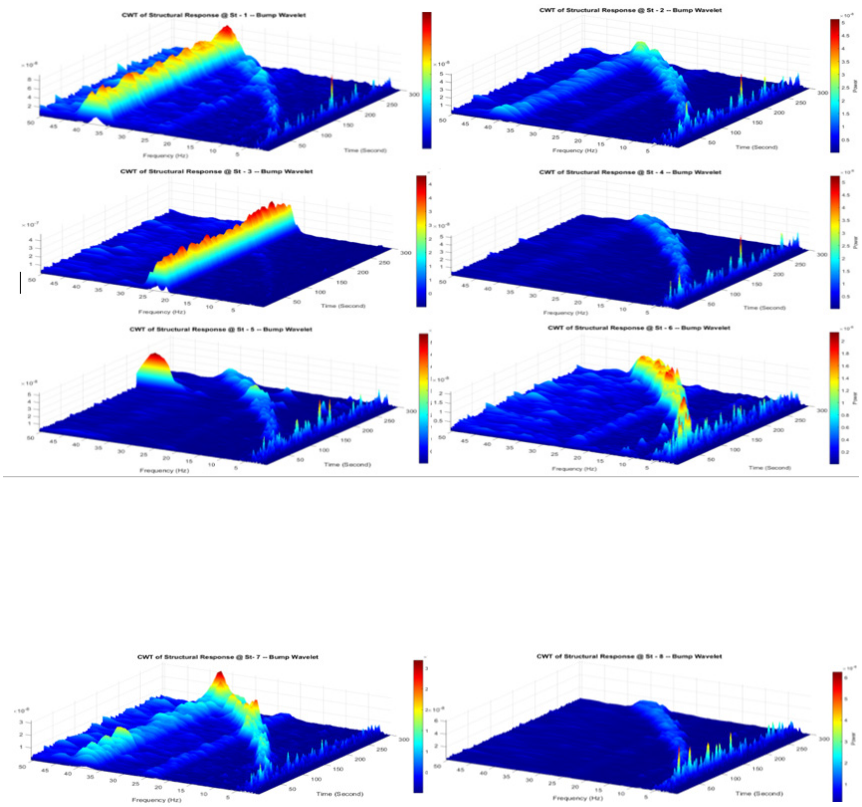

Figure 8 Continuous Wavelet Time-Frequency spectra of the structural observation points of the structure estimated for SE-NW component.

Other stations that generate almost similar energy distributions in T-F domain exhibit nonlinearity-nonstationarity and this tendency increases as the time and frequency progress. Transverse cracks and openings developed around the key block form the hinge mechanism disrupting monolithic behavior and responding individually at its local frequency of 24Hz. Another crown station O_1 also shows close non-monolithic behavior at the local frequency of 38Hz. Other structural members but especially neighbor stations of this low redundant system display nonstationary-nonlinear behavior under the effect of the accumulated damages. Especially neighbor stations O_6 and O_7 located at the springing points of the arch (O_3) are strongly affected. Many types of signals in practice may be non-sparse in the Fourier-based analysis became detectable in T-F domain as seen in Figure 8.

For the Hilbert Huang analysis, EMD technique is applied and leads to physically meaningful decompositions. As we shall see from Figure 9, EMD can extract valuable characteristics of the vibrations with just a few IMF components. IMF with higher frequency content could be identified as being generated by a local instability. After plastic hinge is developed that reduces the level of redundancy and weakens the structural rigidity. As a result, flexibility of the structural system will be increased in a revers manner and this shifts the vibration frequency to lower level. As seen in Figure 9, IMFs start with the highest vibrations and slow down to the small frequency oscillations. Vibrations were developed around the average dominant frequency starting from 38Hz, down to 24Hz, 19Hz, 12Hz, 4Hz, 2.5Hz, 1.5Hz and 1Hz for the first 8 IMFs respectively. Instant T-F spectra of the HHTs for the entire ambient vibrations recorded at the 8 stations are plotted with the peak points in Figure 10. As distinguished from

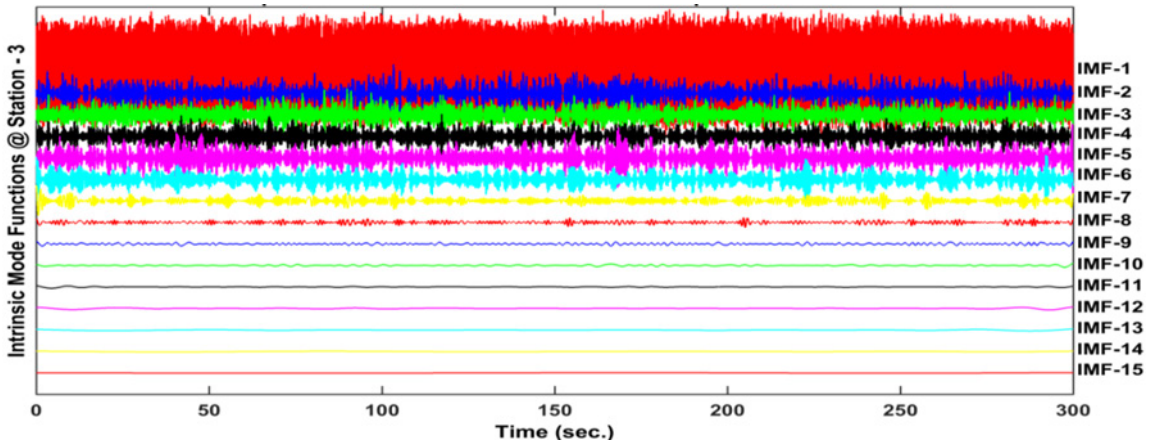

Figure 9. IMFs of the O_3 responses for SE-NW component based on EMD.

Figure 10, some frequencies are never reached in some IMFs. Therefore, zero contribution to the system dynamics from some frequencies can be noticeable.

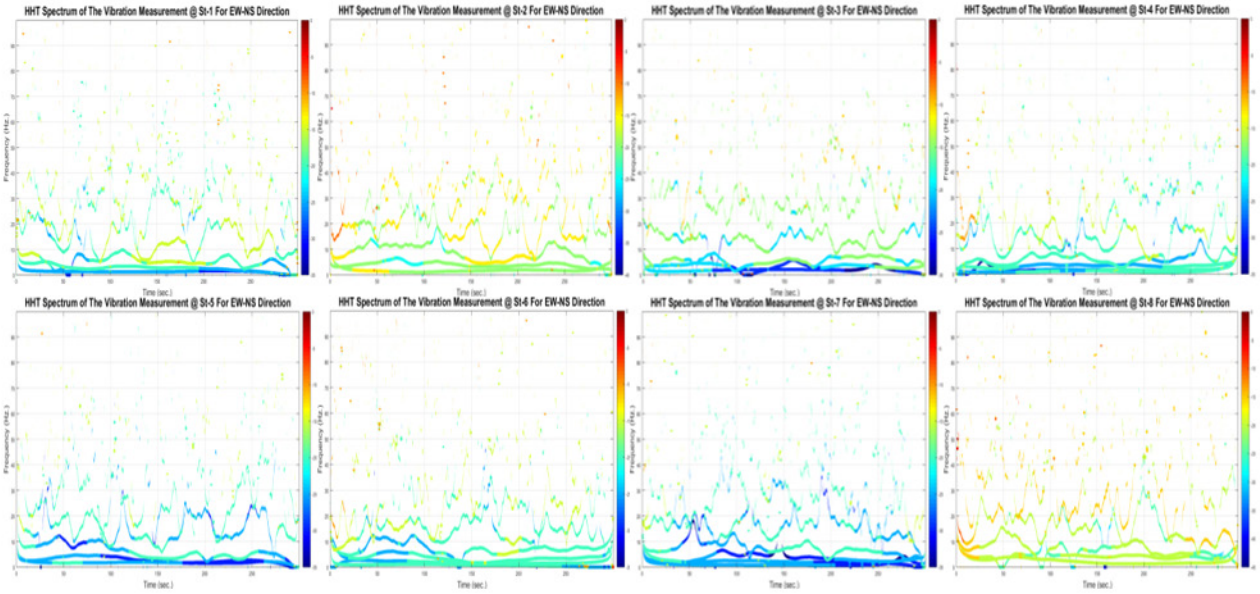

Figure 10. HS peak points of all the IMFs decomposed from 8 stations for SE-NW component. Top four for arch stations (O_1, O_2, O_3, O_4), lower four for column stations (O_5, O_6, O_7, O_8).

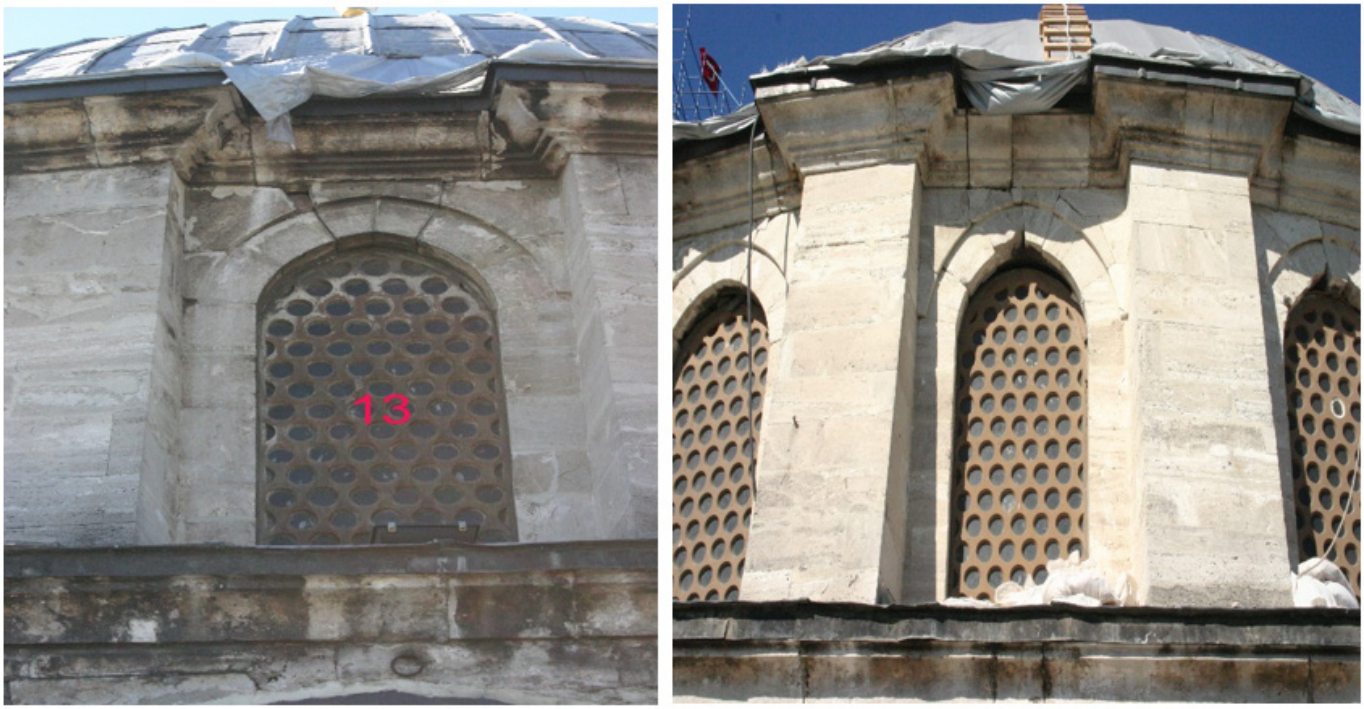

Figure 11 Damage around station 1 (left) damage around station 2 (right) [18, 19].

Figure 12. Damage around station 4 (left), failure cracks on the side dome at station 4 (right) [18, 19].

Fatih Mosque that received damages on several parts by the 17 August 1999 Kocaeli earthquake was repaired widely between 2007 and 2012 [18, 19]. Resultant tension cracks show typical local openings in the window border can be seen respectively in Figures 11 through 14 [18, 19]. In addition to this deterioration, out of plane arch deformations will further degrade the strength capacity. Such strength reductions in the arch system and at the base of the central dome cause distributed deformations and damage. After removing the lead cover, tension cracks in the main dome was observed and large deformations on windows under the main dome base can be also distinguished from the photographs given in the last figures.

Figure 13. Cracks on corner dome at station 5 (left) damage on top of the pillar around the station 6 (right) [18, 19].

Figure 14. Dome damage at the corner around station 7 (left) serious damage at station 8 (right) [18, 19].

7.2. **Structural identification study on a reinforced concrete high-rise building**

In earthquake-prone areas, many tall buildings designed and built according to old building codes can potentially be under earthquake risk. In the literature, the number of studies on the response of tall buildings to large far and near field earthquakes has significantly increased. In recent years, particularly the number of near-field earthquake records was too limited to study the building's responses. There was a lack of knowledge about the tall building behavior during the earthquakes. With the 1995 Kobe earthquake, the 17 August 1999 7.4 Mw Kocaeli earthquake, the 12 November 1999 7.2 Mw Düzce and 1999 Taiwan Chi chi earthquakes, the near-field earthquake archive have enriched. With the new tall building regulations, structural health monitoring provides new data sets. With new collections, tall building responses to near- and far-field earthquakes is attracting great interest and such monitoring appeared as a new area to be studied. In this study, the response of the structure to near and far-field earthquakes, winds and blast forces was investigated in order to understand the characteristics of the structure. The building to be examined was built for residential purposes, and it is instrumented at the three-level as the drawings shows instrumented stories in Figure 15. The events considered as input forces are given in Table 1. In addition to the storm-induced structural acceleration response records, as seen in Table 1, regional earthquakes that occurred in recent years and subway construction explosion recordings were used to understand the structural behavior in this study. Storm-induced building vibrations with a speed of 100Km/h (28m/sec) in acceleration, velocity and displacement forms for the EW direction recorded on floor-34, floor-17 and basement are plotted in figure 16. and a typical near-field earthquake record of acceleration, velocity and displacement time histories are given in Figure 17.

In the signal analysis, the noise that does not contribute to the understanding of the general structural behavior was low pass filtered from the raw data at 0.05Hz and high pass filtered at the Nyquist frequency of 50 Hz., and structure identification was performed. As seen in Figure 18, Fourier transform based Transfer functions are calculated and smoothed by Hanning window for different inputs for the NS direction using the building input output pairs. 0.25 Hz, broad band frequency of 0.8 Hz-1.2 Hz, 2.5 Hz., and 4 Hz., are peak frequencies. In Figure 19, Transfer functions are calculated and smoothed by Kaiser window this time for different inputs for the EW direction. Peak frequencies are seen at 0.25 Hz., 0.8 Hz., and 1.5 Hz. In Figure 20, TFs based on the extra input (feedback) automatic regression (ARX) parametric model are estimated for the (near field earthq.) ML 5.0 Karadeniz earthquake response records, and for the (far field earthq.) ML 5.9 Romania earthquake response records. Far and near field response data yield same peak frequencies 0.25 Hz and 0.9 Hz in the EW direction. and about 0.42 Hz and 1.6 Hz. in the NS direction.

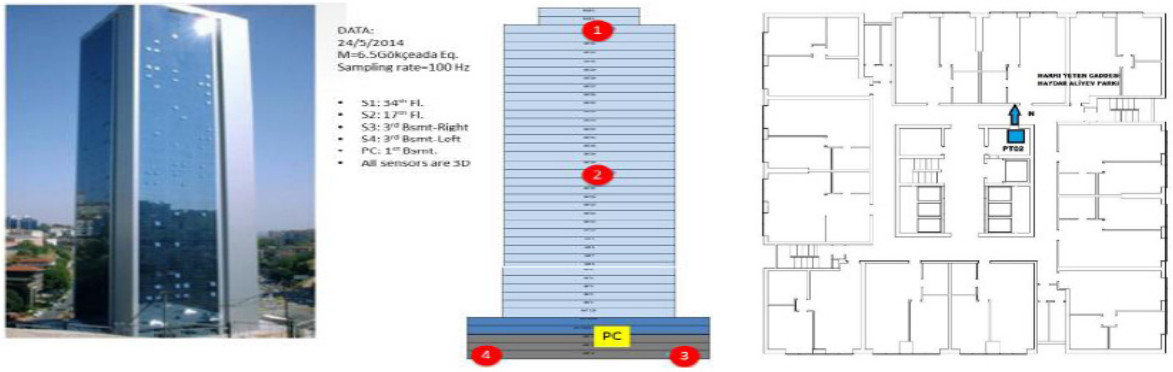

Figure 15. General view of the high-rise building and the positions of the 3-component accelerometers at the basement, 17th and 34th Floors along the height of the building and their locations in the normal floor plan.

Table1. Dynamic Forces (events) considered in this study

No	Date (yyyyaagg)	Time (Local)	Time (İnternational)	Latitude (degree)	Longitude (degree)	Depth (km)	Size (ML)	Distance (km)	Location
1	20130730	08:33:08	05:33:08	40.3037	25.7830	9.8	5.3	287	Kaleköy-Gökçeada
2	20131124	22:49:37	19:47:39	40.7843	31.876	8.0	4.8	240	Ulu Mosque (Bolu)
3	20131127	06:13:37	04:13:37	40.851	27.9198	9.6	4.7	96.6	Marmara Spans (Tekirdağ)
4	20140130	04:54:33	02:54:33	40.6733	29.2688	8.5	3.1	49.89	Yalova
5	20140205	03:56:43	01:56:43	41.3768	28.622	16	3.8	46.0	Karaburun-Arnavutköy
6	201441122	21:14:15	19:14:15	45.742	27.2147	27.9	5.6	526.0	Romania
7	20150117	02:42:34	00:42:34	39.8848	30.3955	5.5	4.3	175.0	Karaçoban Pınarı Eskişehir
8	20150119	13:10:43	11:10:43	40.8648	27.6787	16	3.0	40.3	Marmara Sea
9	20150122	18:47:04	16:47:04	40.6233	29.1082	12.3	2.5	51.0	Çınarcık (Yalova)
10	20150123	12:19:42	10:19:42	40.0647	28.587	5.0	4.5	119.0	Uğurlupınar (Bursa)
11	20150201	12:46:31	10:46:31	40.7125	27.4973	6.0	3.5	135.0	Güzelköy-Tekirdağ
12	20150202	06:41:03	04:41:04	40.3412	26.0567	13.4	4.1	364.0	Soros Bay (Ege Sea)

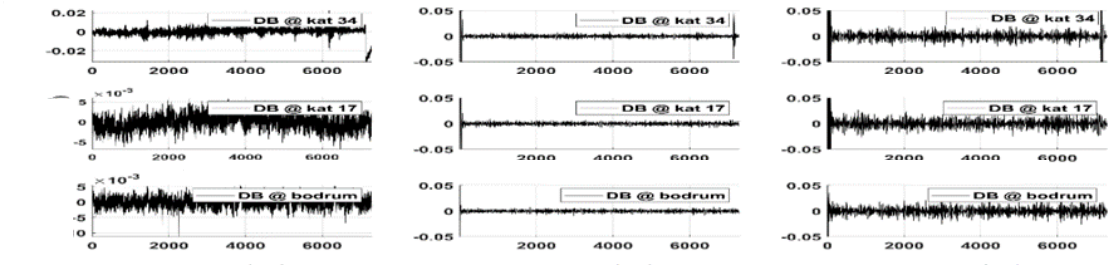

Figure 16. Acceleration responses of the tower to storm in EW direction

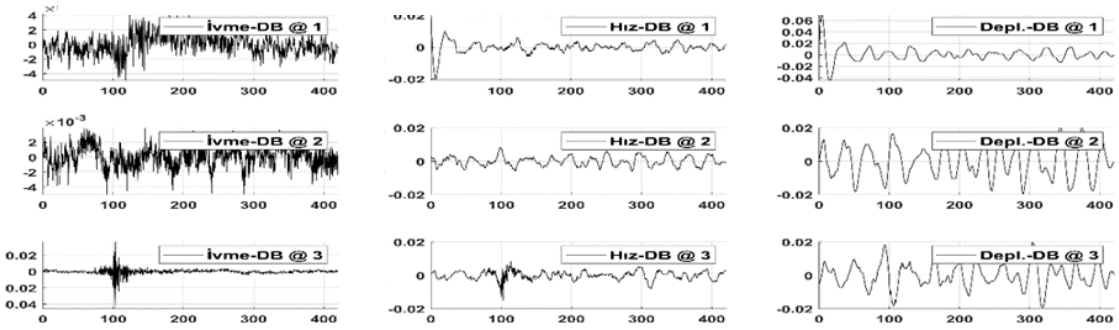

Figure 17. EW component acceleration, velocity and displacement time histories of the 2016-10-15 5.0 ML Karadeniz earthquake recorded on floors 34, 17 and basement

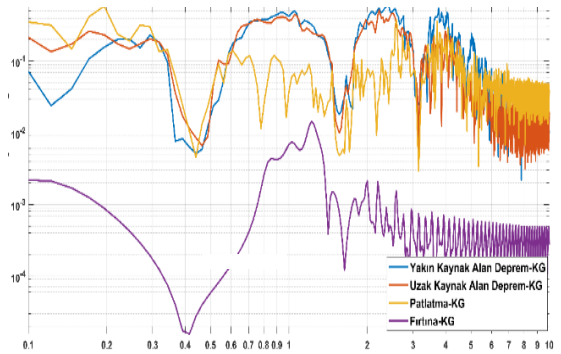

Figure 18. TF for NS component of the different ınput responses at floor 34

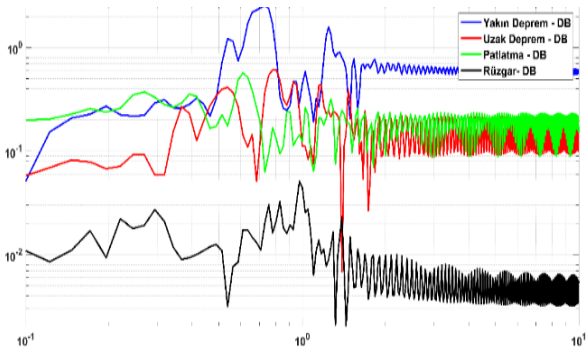

Figure 19. TF for EW component of the different ınput responses at floor

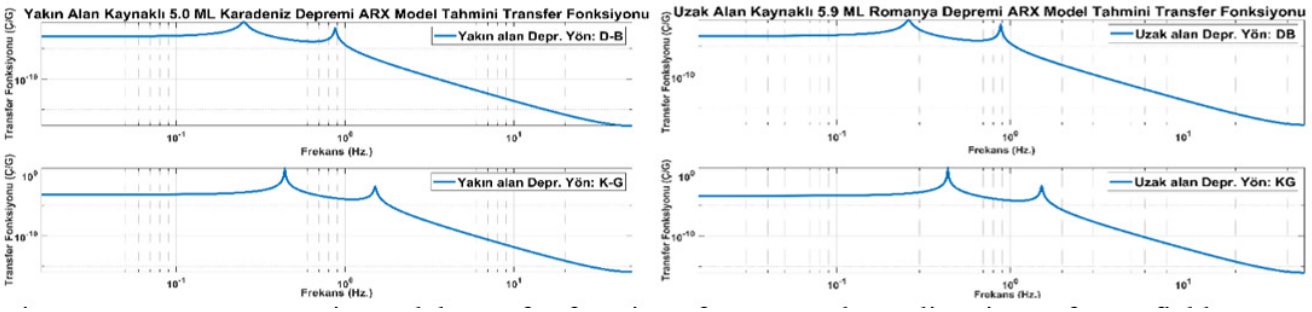

Figure 20. ARX parametric model transfer functions for EW and NS directions of near field 5.0 ML Karadeniz (left) and far field 5.9 ML Romania earthquakes (right) responses of the 34th floor.

In State-Space (SS) domain, using OKID-ERA for the NS response component of the ML 5.9 20161228 Romania earthquake, TF is calculated and plotted in Figure 21. Detectable peak frequencies are 0.25 Hz., 0.42 Hz., 0.61 Hz., 1 Hz. 1.6 Hz. and 3.1 Hz., respectively. But peak frequency of 3 Hz cannot be reached from explosion data. It is seen clearly that the global peak responses are obtained very closely from different input sources. In the EW direction, the natural dominant frequencies of the structure are 0.25Hz, 0.9Hz; It can be said that the global response peaks are observed at 0.4Hz, 1.4Hz and about 3Hz in the NS direction.

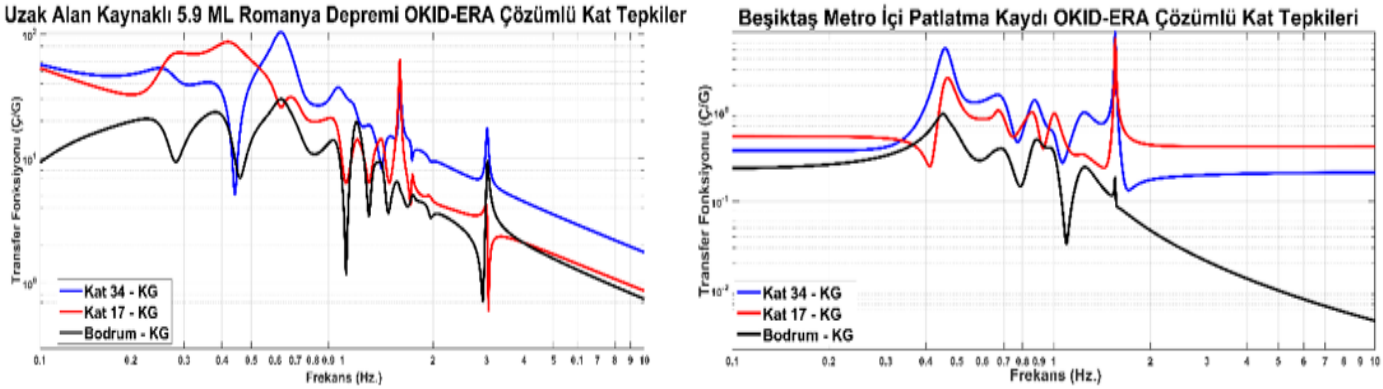

Figure 21 OKID-ERA results for 5.9 ML Romania earthquake (left) and for explosion response (right)

In addition, wavelet analyzes were carried out using the appropriate mother wavelet family after performing some tests to select the best one among the several candidates. Resultant wavelet spectrum is plotted in Figure 22 for the EW responses of the near and far field data recorded at the top story of the tower. Data set are the collection of near field 5.0 ML Karadeniz earthquake and far field 5.9 ML Romania earthquake. As observed, global response frequency of the tower is not changing and produces its peak at the frequency of 0.42 Hz. Another important information that can be gained from these wavelet spectra is the time location of the fundamental peak. It shows that the far field data should be recorded much longer than the near field earthquakes. Dominant peak is seen at about 145 second in the near field data and at 260 second in the far field data. Another wavelet analysis performed for the explosion caused responses during subway tunnel construction and it is plotted in Figure 23. Wavelet spectrum of the explosion response shows that the initial response of the explosion in NS direction starts approximately at 4 second within the frequency band of 0.43 Hz-0.75 Hz. After structural response initiated, wave fronts with low energy propagates in a P wave propagation form through the structure up to the tip of the tower with a central frequency of 0.42 Hz. This P wave form propagation is observed as tension-compression wave fronts in the 34th floor response history through the record length of 180 seconds. In the EW direction, top floor of the tower receives oscillations at the central frequency of 0.22 Hz. and 0.4 Hz. within the form of shear wave, which is perpendicular to longitudinal propagations observed in NS direction. Figure 24 is the results of the Hilbert-Huang Transform (HHT) of the 3.8 ML magnitude Karaburun Arnavutköy İstanbul earthquake. It is understood that the frequency variations of the tower show the linear stationary characteristic throughout the record length for far and near field earthquakes, blast and storm induced vibration responses.

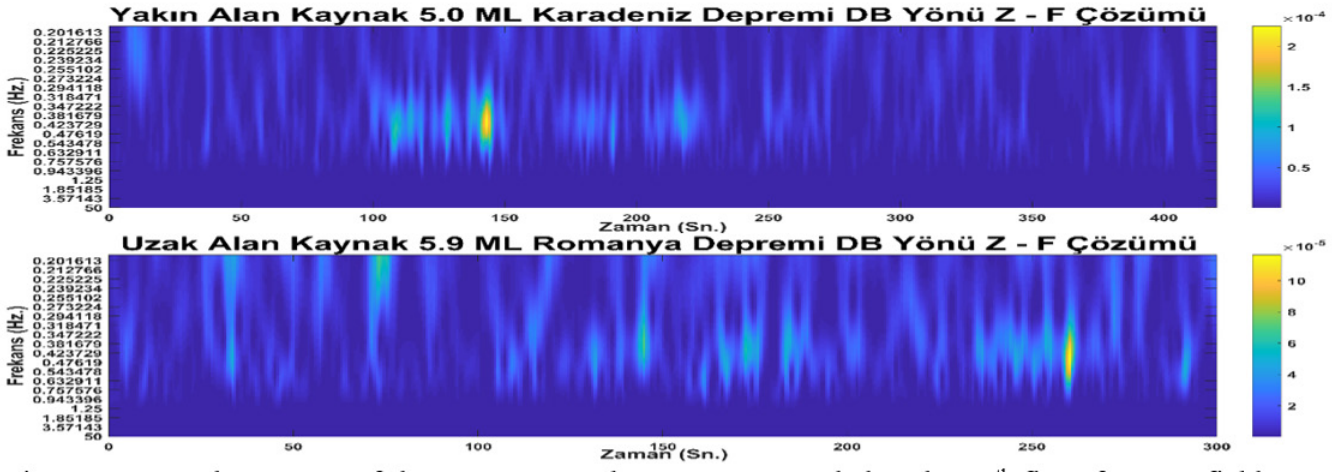

Figure 22. Wavelet spectra of the EW structural responses recorded at the 34th floor for near field 5.0 ML Karadeniz earthquake (top) and far field 5.9 ML Romania earthquake (bottom).

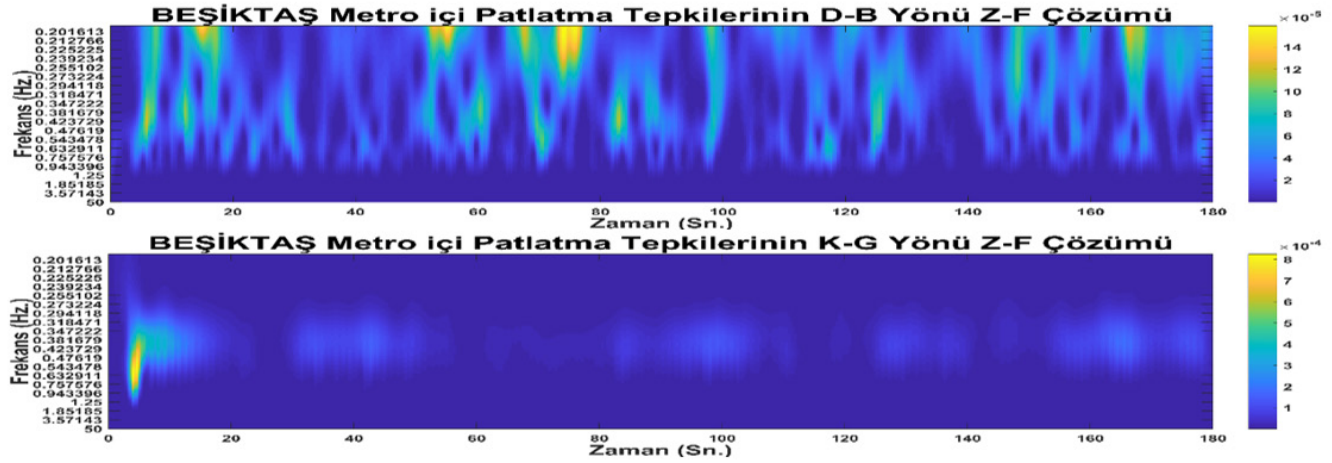

Figure 23. Continuous wavelet transformation spectra of the 34th floor EW response to subway explosion (Beşiktaş) (top) and NS (bottom)

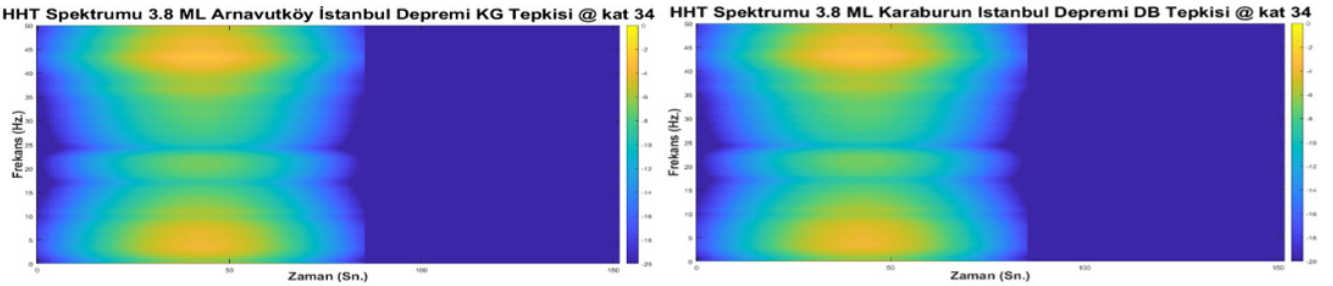

Figure 24. HHT spectra of the near field earthquake response during the 3.8 ML Arnavutköy earthquake recorded at the 34th story, for NS direction (left) and EW direction (right)

8. Conclusions

This paper as a state of the art and practice in the damage detection presents a brief review of different damage identification and system identification methods and their applications to the civil engineering structure. Applying spectral and parametric methods, results show that modal features can be extracted thoroughly, but damage detection is not explicitly performed. Analyses were extended to T-F decomposition in order (1) to describe how the spectral content of the signal changes with time; (2) to verify the effectiveness of the T-F analysis in damage identification in case of ambient vibration recordings and (3) to discuss comparably well sides and significant doubts on the suitability of the techniques in damage identification studies. STFT, WT and HHT utilized as different vehicles were discussed to reexamine superior performance of the suitable one with some advantageous. Finally, useful quantitative information that was extracted from WT and HHT has achieved very close results about the damage and time varying spectral characteristics. On the other hand, since structural damages do not allow the structure to behave in a monotonic fashion, results of the different analysis methods in either way yield similar results but ignorable small differences in frequency content. For light redundant structures, there is a need to develop automatic signal/image processing to identify anomaly through image processing, machine vision, and pattern recognition. Ambient measurement data has enough sensitivity for advanced damage identification and adequately captures nonlinear nonstationary characteristics.

In another application, the structural health monitoring network installed on a high-rise building summarizes the estimation of the

building characteristics with different methods by using the response of the building to the input forces of different sources in the building identification studies. It is seen that all these natural forces are not alternative to each other. As observed in the nature, the frequency contents, which may change from low to high and may be reach or poor, complete the structural information to be extracted for better understanding the dynamic properties of the engineering structure. In addition, tracking of the results obtained from the building health monitoring network constitutes an important archive for the detection of anomalies. Time Frequency analysis may affect and improve the building codes for a risk consistent structural design. The future revisions of aseismic design and condition assessment methodologies will use the time-frequency domain analysis to better understand the chaotic natural forces and their responses. Time-Frequency analysis that promises new horizons will affect and improve the current procedures, check points and limits to artificially generate the seismic ground motions or evaluate the recorded strong ground motions for the time domain analysis.

Declaration of Conflict of Interests

I declare that this did not work there is no conflict of interest.

References

[1] Turkish Earthquake Building Code, 2018, AFAD.

[2] Beyen, K. (2021), Damage Identification Analyses of a Historic Masonry Structure in T-F Domain, Teknik Dergi, 2021 10577-10610, Paper 604.

[3] Ewins, D. J. (2000), Adjustment or Updating of Models, International Winter School on Optimum Dynamic Design Using Modal Testing and Structural Dynamic Modification, Indian Academy Sciences, 235-245.

[4] Farrar, C. R., Doebling S. W., Cornwell, P. J., and E. G. Straser (1997), "Variability of modal parameters measured on the Alamosa Canyon Bridge", in Proc., 15th Int. Modal Analysis Conf., Orlando, FL.

[5] Beyen, K. (2008), "Structural Identification for Post-Earthquake Safety Analysis of the Fatih Mosque after the 17 August 1999 Kocaeli Earthquake", Engineering Structures, 30.

[6] Inman, D. J. and Minas, C. (1986), "Matching analytical models with experimental modal data in mechanical systems", Control and Dynamics Systems, Vol. 37, 327-363.

[7] Bendat, J. S. and Piersol, A. G. (2004), Random Data, Analysis and Measurement Procedures, JW, USA.

[8] Bendat, J. S. (1990), Nonlinear System Analysis and Identification from Random Data, Wiley-Interscience, USA.

[9] Huang, N. E., Zheng, S., Long, S. R., Wu, M. C., Shih, H. H., Zheng, Q., Yen, N.-C., Tung, C. C., and Liu, H. H. (1998), "The empirical mode decomposition and Hilbert spectrum for nonlinear And nonstationary time series analysis." Proc. R. Soc. London, Ser. A, 454.

[10] Bo Chen, Sheng-lin Zhao, and Peng-yun Li, ' Application of Hilbert-Huang Transform in Structural Health Monitoring: A State-of-the-Art Review ', Hindawi Publishing Corporation, Mathematical Problems in Engineering Volume 2014, Article ID 317954, 22 pages, http://dx.doi.org/10.1155/2014/317954.

[11] B. Vincent, J. Hu, and Z. Hou, "Damage detection using empirical mode decomposition and a comparison with wavelet analysis," in Proceedings of 2nd International Workshop on Structural Health Monitoring, pp. 891–900, Stanford Univeristy, Stanford, Calif, USA, 1999

[12] J. N. Yang, Y. Lei, and N. E. Huang, "Damage identification of civil engineering structures using Hilbert-Huang transform," in Proceedings of the 3rd International Workshop on Structural Health Monitoring, pp. 544–553, Stanford, Calif, USA, 2001.

[13] Catbas, F.N., KijewskiCorrea, T. and Aktan, A.E. (2012). Structural Identification of
Constructed Facilities: Approaches, Methods, and Technologies for Effective Practice of
StId , ASCE, Reston, VA. USA.

[14] Juang, J. N. (1994), "Applied System Identification", Prentice Hall, Englewood Cliffs, New Jersey.

[15] Juang, J. N., Pappa, R. S. (1985), "An Eigen system Realization Algorithm for Modal Parameter Identification and Model Reduction", J. of Guidance, Control and Dynamics, 8, No.5.

[16] Mathworks (2019), Signal Processing Toolbox for Matlab, Release 2019b, The MathWorks Inc., Natick, MA.

[17] Chen, H.P. (1998) Structural Damage Identification Using Vibration Modal Data. PhD thesis, Department of Civil Engineering, Glasgow University, UK.

[18] Yılmaz Yapı Taah. Ve Tic. Ltd. Şti. Özel Fatih Camii Restorasyon Arşivi, 2019.

[19] Fatih Sultan Mehmet Camii ve Sultan I. Mahmut Kütüphanesi Restorasyonu (2008-
2012), 2019, Yılmaz Yapı Taah. Ve Tic. Ltd. Şti. Yayınları, (baskıya hazırlanıyor in
press).

Biography

Born in Istanbul in 1960, undergraduate from Yıldız Technical University in 1985 and graduated from institute of science - civil Engineering department of same university in 1989. Those years I practiced as a civil engineer. I graduated from Boğaziçi University-Kandilli Observatory and Earthquake Research Institute, earthquake engineering department as an earthquake engineer doctor. Between 1989 and 2004, I assisted many undergraduate and graduate courses in earthquake engineering department. I was involved in various projects, construction sites, structures and field-testing studies for the last 30 years. Structural dynamic tests, structural health monitoring, strong ground motion recorder and monitoring network development, signal processing, structural identification, and advanced nonlinear dynamic analysis, damage identification analyzes in time-frequency domain with nonstationary and nonlinear simulations are my recent subjects.